General Disclaimer

One or more of the Following Statements may affect this Document

- This document has been reproduced from the best copy furnished by the organizational source. It is being released in the interest of making available as much information as possible.

- This document may contain data, which exceeds the sheet parameters. It was furnished in this condition by the organizational source and is the best copy available.

- This document may contain tone-on-tone or color graphs, charts and/or pictures, which have been reproduced in black and white.

- This document is paginated as submitted by the original source.

- Portions of this document are not fully legible due to the historical nature of some of the material. However, it is the best reproduction available from the original submission.

TECHNICAL REPORT STANDARD TITLE PAGE

1. Report No.	2 Government Accession No	3 Recipient's Catalog No.

4 Title and Subtitle

THE OSU SELF-PHASED ARRAY FOR PROPAGATION MEASUREMENTS USING THE 11.7 GHz CTS BEACON

5 Report Date
November 1976
6 Performing Organization Code

7. Author(s)
D. M. Theobold and D. B. Hodge

8 Performing Organization Report No
ESL 4299-1

9. Performing Organization Name and Address
The Ohio State University ElectroScience Laboratory, Department of Electrical Engineering, Columbus, Ohio 43212

10 Work Unit No

11 Contract or Grant No
NAS5-22575

13 Type of Report and Period Covered
Type II
Technical Report

12. Sponsoring Agency Name and Address
NASA, GSFC
Greenbelt, Maryland 20771
E. Hirschmann, Code 951, Technical Officer

14 Sponsoring Agency Code

15. Supplementary Notes

16. Abstract

This report describes the self-phased array developed by the Ohio State University ElectroScience Laboratory for propagation measurements on an earth-space path. The 11.7 GHz CTS beacon is used as the signal source in the current measurements. The self-phased array is used to measure angle-of-arrival as well as attenuation and scintillation statistics. The performance of the array is described and sample data are presented.

As a subsidiary result, the tracking capability of the self-phased array is also presented. This technique permits fully-electronic, non-mechanical satellite tracking, thus simplifying unmanned operation and eliminating severe weather tracking constraints.

17. Key Words (Selected by Author(s))

Propagation
Millimeter Wave
Angle-of-arrival
Attenuation
Self-phased array
Scintillation

18 Distribution Statement

19. Security Classif. (of this report)	20. Security Classif. (of this page)	21. No. of Pages	22. Price*
U	U	23	

*For sale by the Clearinghouse for Federal Scientific and Technical Information, Springfield, Virginia 22151.

CONTENTS

I. INTRODUCTION

The effort described herein represents the initial phase of the Ohio State University's participation in the NASA CTS Communications Link Characterization Experiment. The objective of the Ohio State University CTS angle-of-arrival experiment is to measure angle-of-arrival, attenuation, and scintillation statistics on a millimeter wavelength earth-space propagation path and, as a secondary objective, to assess the performance of a self-phased array utilized for non-mechanical tracking in an earth-space communication link. This experiment utilizes the 11.7 GHz Beacon on the synchronous Communications Technology Satellite (CTS). The ground terminal utilized in this experiment is located at the Ohio State University Satellite Communications Facility in Columbus, Ohio.

The CTS 11.7 GHz beacon characteristics will be discussed and the influence which these parameters have on the experiment design will be presented. The experimental implementation will be described and system performance will be demonstrated with measured data. Finally, measured propagation data will illustrate examples of precipitation fade and scintillation events. Some of the data contained in this report were also presented in Reference [1].

II. CTS 11.7 GHz BEACON CHARACTERISTICS

The CTS beacon transmits a 200 mw cw signal at 11.7 GHz. The short term amplitude stability of this signal is ±0.1 dB/hour and the long term amplitude stability is ±1.5 dB/year. The long term frequency stability of the beacon was estimated at 1 part in 10^6 per month. Additionally, maximum doppler shifts of ±650 Hz corresponding to maximum radial velocities of ±12 km/hr were expected. The amplitude stability of the beacon is quite acceptable for the measurement of absolute fade statistics, but the frequency instability and doppler shift require frequency tracking of the phase lock receivers, which will be considered in the next section.

The spacecraft is maintained on geosynchronous station to within ±0.2° longitude. Inclination is not controlled and is nominally 0.9°. The Columbus terminal, located at 83.0417 E longitude and 40.0028° N latitude, has nominal look angles of 225.3° azimuth and 32.7° elevation for the satellite. Predicted diurnal look angle variations are ±0.4° in azimuth and ±0.25° in elevation. Figure 1 illustrates a typical twenty-four hour plot of the satellite motion. Superimposed on this plot are constant gain levels for a single antenna element of the self-phased array.

The amplitude, frequency, and orbital characteristics directly influence the angle-of-arrival experiment design. These considerations and the experimental implementation will now be described.

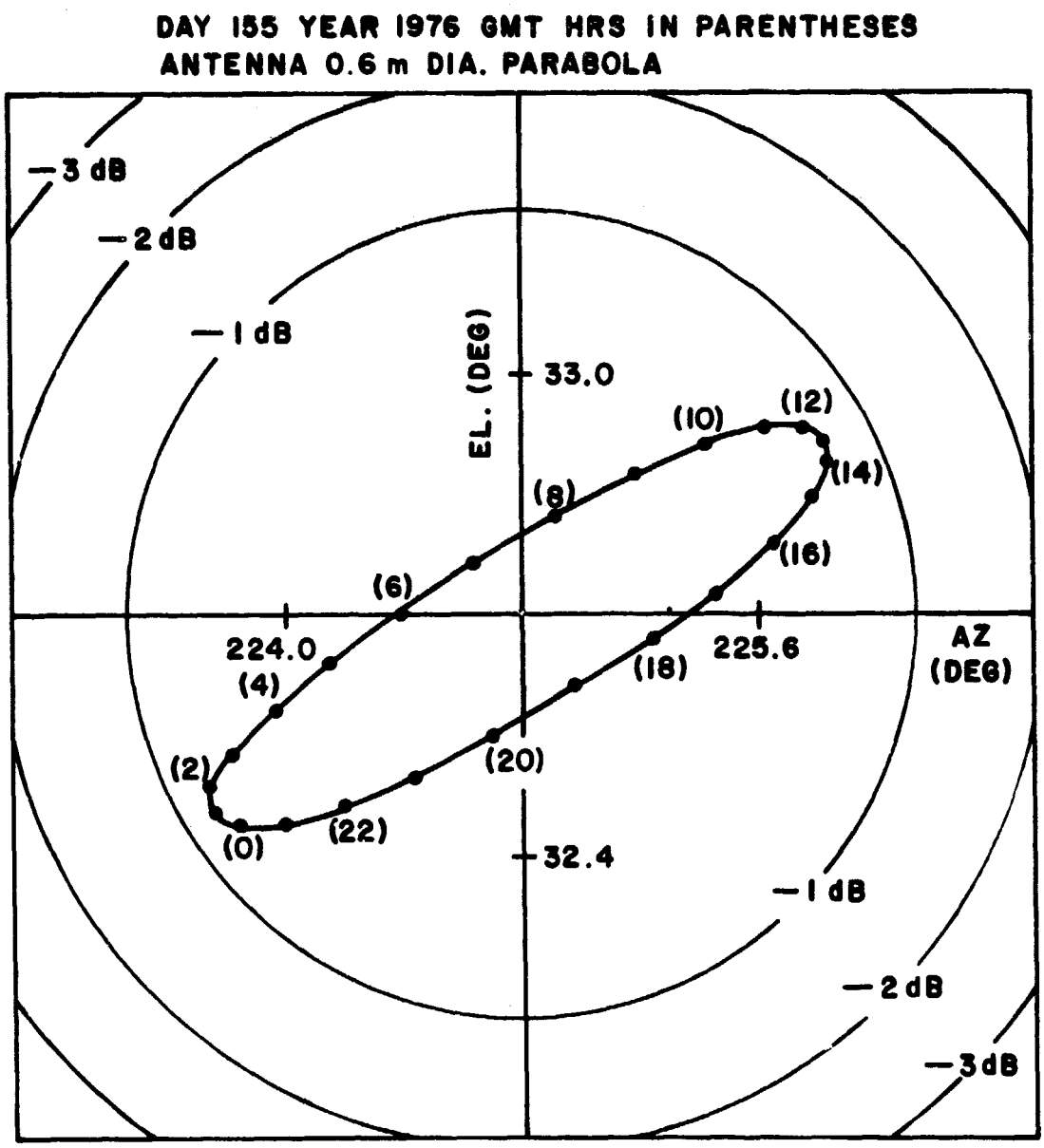

Figure 1. Diurnal satellite motion and array element antenna pattern.

III. DESIGN AND IMPLEMENTATION

The two primary considerations in the design of the system were angle-of-arrival measurement capability and reliability of unattended operation. Both have been satisfied by implementing a self-phased array whose antenna elements were chosen to have individual beamwidths wider than the diurnal motion of the satellite. The angle-of-arrival in a plane containing the propagation path may be related to the differential phase between two elements of the self-phased array located in that plane. By using four elements (Figure 2), one obtains

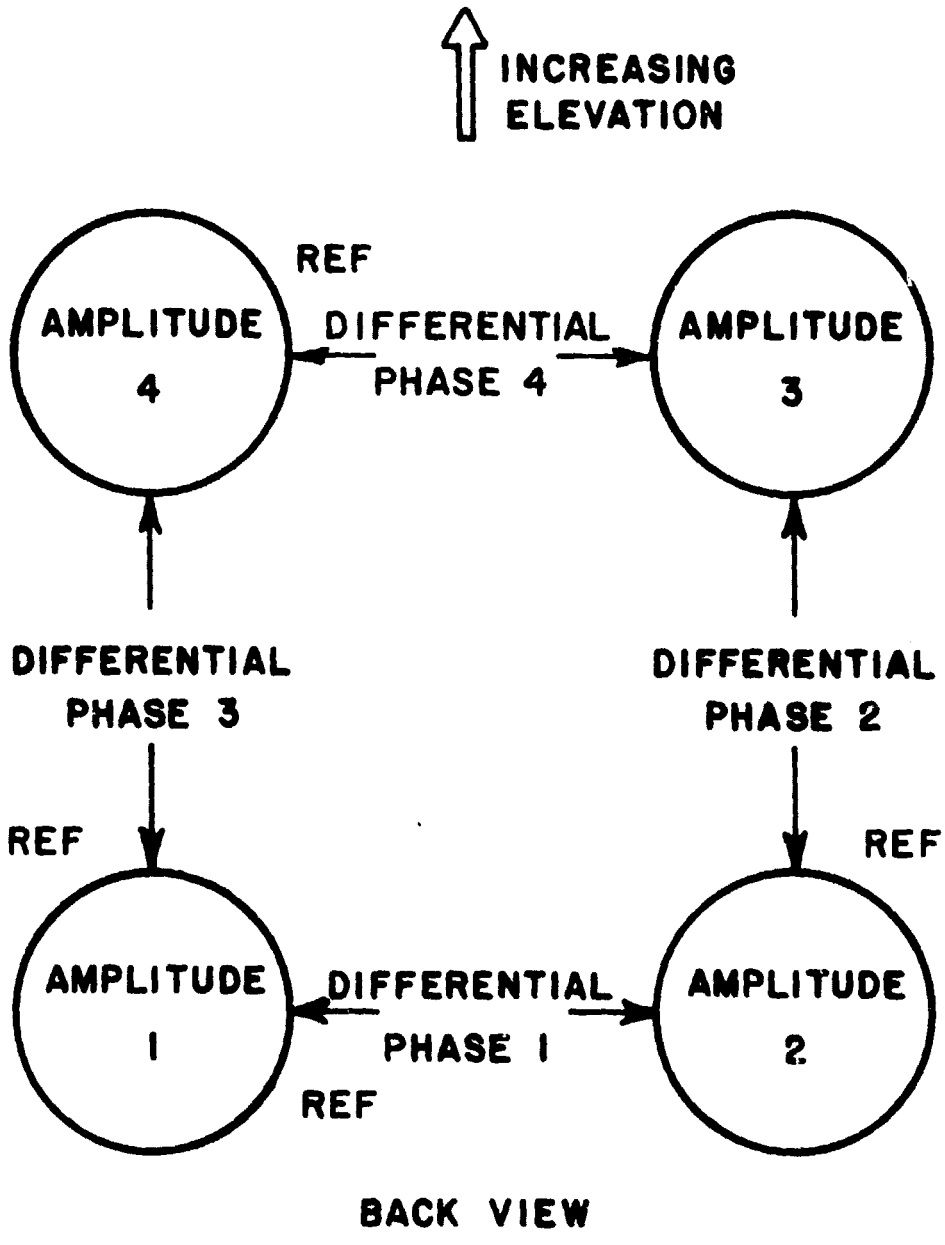

Figure 2. Self-phased array configuration.

two independent angle-of-arrival measurements in each of two orthogonal planes, i.e., differential phases 1 and 4 in the azimuth plane and phases 2 and 3 in the elevation plane.

Each parabolic element is 0.6 m in diameter, giving a 3° beamwidth at 11.7 GHz (see Figure 1). Left-hand-circular-polarization (LHCP) focal point antenna feeds are used to obtain maximum signal from the satellite, which transmits RHCP. The elements are mounted on a planar surface with center-to-center spacing of 1.0 m. An elevation-over-azimuth mount serves as a base for the array and is fixed-pointed, with the self-phased array providing automatic beam tracking. Hence, the automatic tracking allows unattended operation. The system is shown in Figure 3.

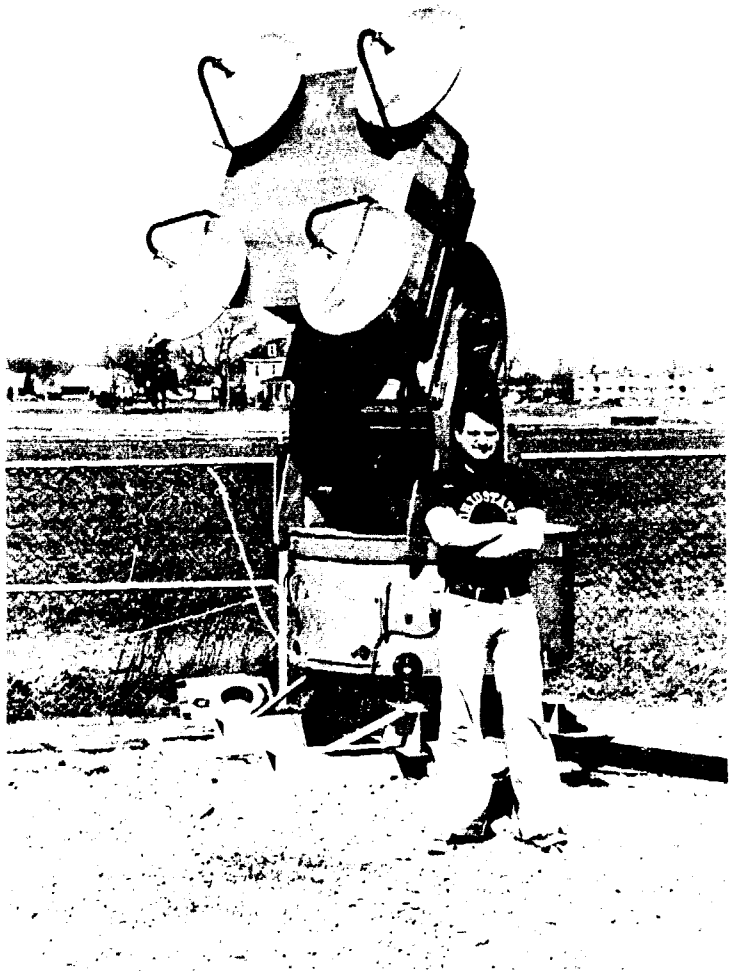

Figure 3. CTS self-phased array.

The 0.6 m element aperture size was a result of the following constraints; first, the aperture must be small enough, i.e., the beamwidth large enough, that adequate gain is maintained as the satellite goes through its diurnal motion, second, the aperture must be small to reduce measurement error due to phase averaging over the aperture, and third, the aperture must be large enough, i.e, the gain must be high enough, to provide an adequate signal-to-noise ratio for the measurement. The 1.0 m element spacing was a result of the constraint that the spacing must be large enough to provide reasonable angular resolution and yet small enough to reduce ambiguity problems associated with large differential phase excursions.

The self-phased array receiver (Figure 4) aligns the phase of the signal from each element with that of a reference signal common to all elements. The reference is a precision 455 KHz crystal oscillator with one part in 10^8 accuracy. After phase alignment, the four signals are coherently summed, giving an array gain of 6 dB over that of a single element. Figure 5, a plot of a representative probability density function of amplitude variance for one array element and the array sum, demonstrates this improvement in signal-to-noise ratio. The mean of the variance for the array sum is approximately 6 dB below that of the individual element.

The phase-lock-loops, which provide phase alignment for the elements, control the receivers with 2.545 MHz VCXO mixer injection. These VCXO outputs are also used to derive the inter-element differential phase measurements from which angle-of-arrival is determined. This is possible because all downconversions prior to the 2.545 MHz injection are common to the four elements (for details, see Appendix I). The 2.545 MHz outputs are compared with phase detectors referenced according to Figure 2. The unambiguous output range of the phase detectors is ±90°. To resolve ambiguities for larger differential phase, the VCXO control voltages are also monitored (Figure 4, outputs 9-12). The digital data system can detect changes as small as 39 mv, corresponding to 0.7° in differential phase and 70° in the VCXO phase; thus, any ambiguity in phase can be resolved.

The first downconversion to 30 MHz is made by injecting 11.67 GHz common to all elements. This signal is obtained from a phase-lock outer control loop referenced to one receiver element. This outer loop tracks out doppler frequency and satellite oscillator drift (see Appendix I for detail). Because the outer loop control is common to all elements, it does not affect the differential phase measurements.

Amplitude detection at each element and on the coherent sum channel is performed at 455 KHz. The 455 KHz bandwidth is 80 Hz and the system margin per element is 19 dB. The digital data system can detect amplitude changes on the order of 0.1 dB.

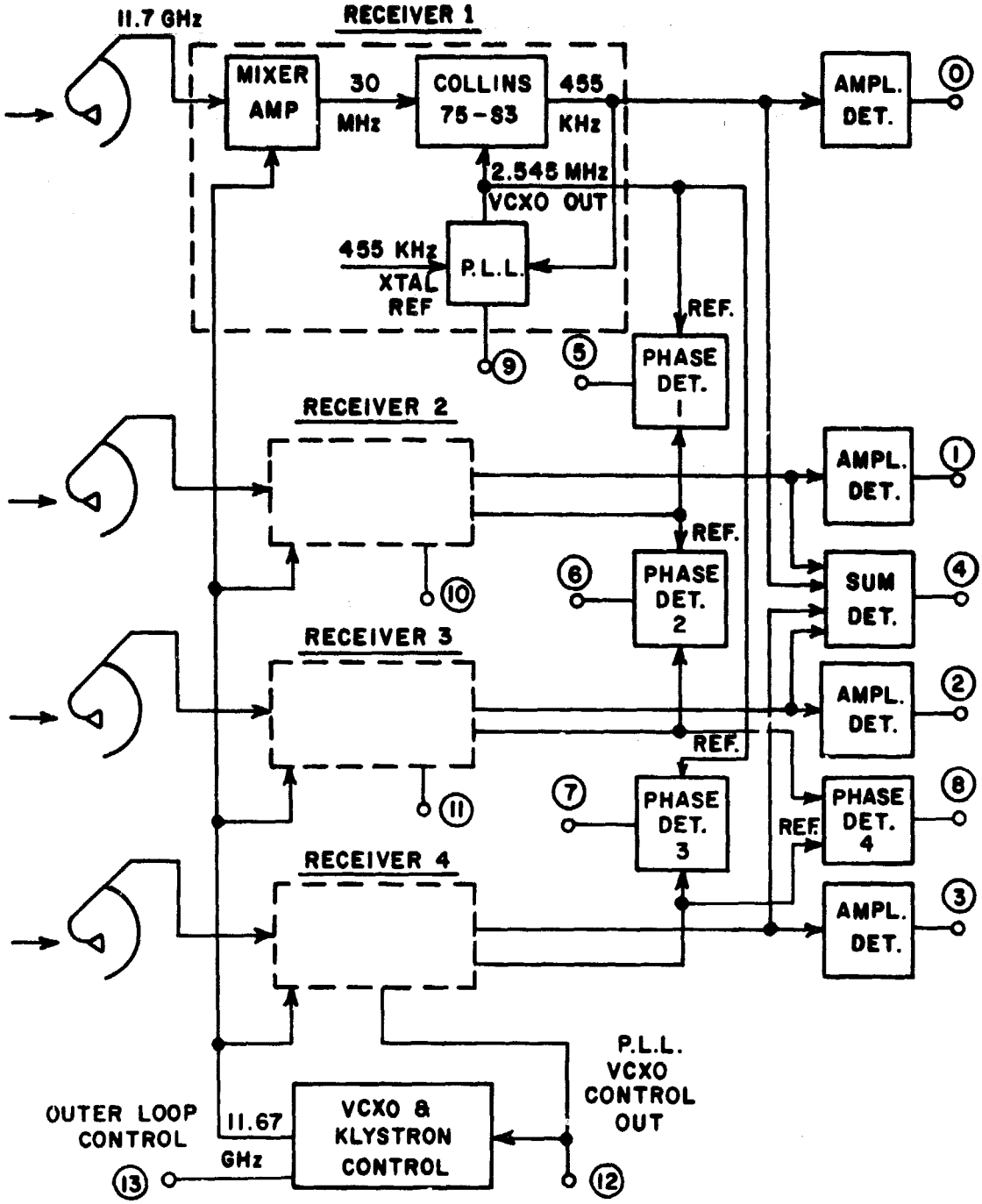

Figure 4. Self-phased array receiver block diagram.

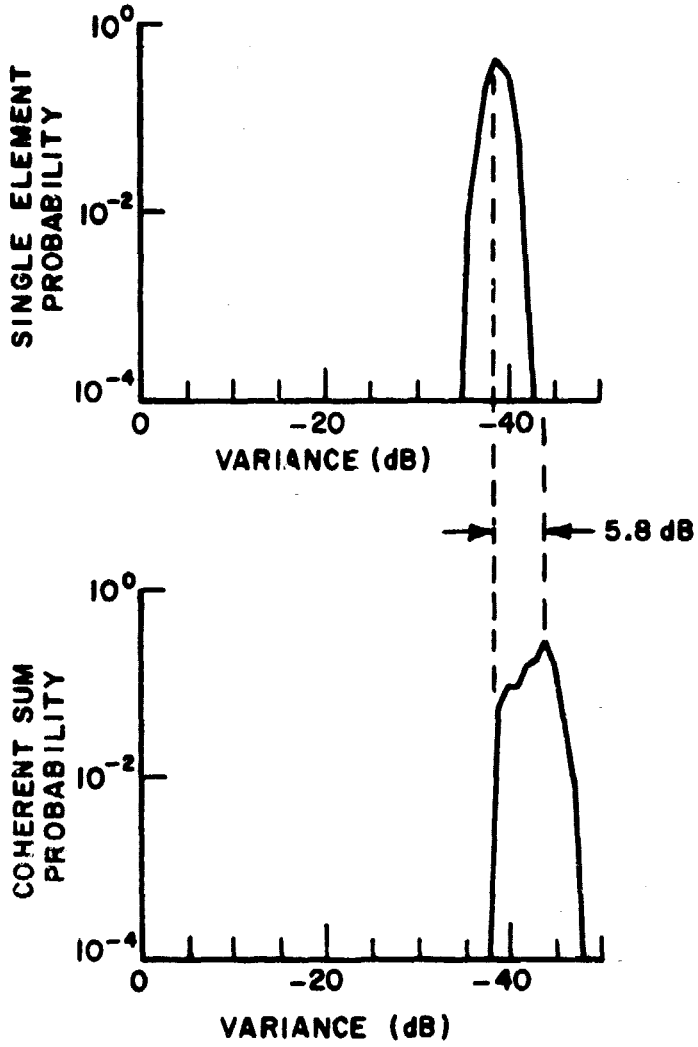

Days 188-191
Sample Rate 1/3 sample/sec.
3000 minute data base
32 sample increment
Variance increment 0.5 dB

Figure 5. Amplitude channels - variance probability density functions.

All data are multiplexed, A/D converted, buffered, and recorded on digital magnetic tape. The data system is described in detail in Reference [2]. The record type and format for CTS data is presented in Appendix II. All channels are sampled at a rate of 1/3 samples/sec at all times. A sample rate of 10 samples/sec can be demanded manually for particularly interesting events.

IV. PERFORMANCE

Two examples will be used to demonstrate the performance of the self-phased array receiver. The first involves moving the array to produce amplitude and phase patterns and the second examines the array output as the satellite undergoes its diurnal motion with the array fixed.

In Figure 6 the array has been moved off the propagation path in azimuth at time 0.0 min., is slewed through its pattern maximum at 1.1 min., and is off the path again at 2.2 min. Note that amplitude channel 1 represents the single element pattern. $\Delta\phi 1$ is an azimuth differential phase output. The azimuth differential phase undergoes progressive 90° shifts as the array axis passes through the propagation path.

Using elementary array theory, if d is the distance between two elements and α is the angle-of-arrival measured from the axis of the array, the differential phase between the elements is:

$$\Delta\phi = kd \sin \alpha \ , \qquad (1)$$

where $k = 2\pi/\lambda$ is the usual propagation constant. For the case shown in Figure 6, the azimuth, α, has varied from -2.45° to +2.45° and, therefore, the total phase excursion is 1,200°. Since $\Delta\phi 1$ undergoes about 14 multiples of 90°, or 1260°, the array is indeed measuring angle-of-arrival in the azimuth plane. $\Delta\phi 2$ and $\Delta\phi 3$, measures of elevation differential phase, remain relatively constant in phase as the array moves in azimuth, as is expected. Any change from constant phase may be attributed to misaligned antenna feeds or non-orthogonal baselines between elements.

Figure 7 is a similar amplitude and phase pattern taken in the elevation plane. This time the azimuth measurement $\Delta\phi 1$ remains relatively constant while the two elevation differential phases $\Delta\phi 2$ and $\Delta\phi 3$ undergo phase changes as the elevation pattern is run. Again, $\Delta\phi 2$ and $\Delta\phi 3$ undergo approximately 1260° of change for an elevation change of 4.9°.

The second example (Figure 8) examines measured azimuth and elevation differential phases over a 24 hour period. Predicted look angles are also plotted above the measured data. Note that the self-phased array tracks the diurnal satellite motion quite well. Two points of interest may be noted. An inflection point occurs in the azimuth differential phase at hour 19 due to foldover in phase. Also, there is some time skew for both pairs at the hour 12 cross-over points. Both conditions are attributed to the fact that the axis of the array was not centered on the diurnal pattern of the

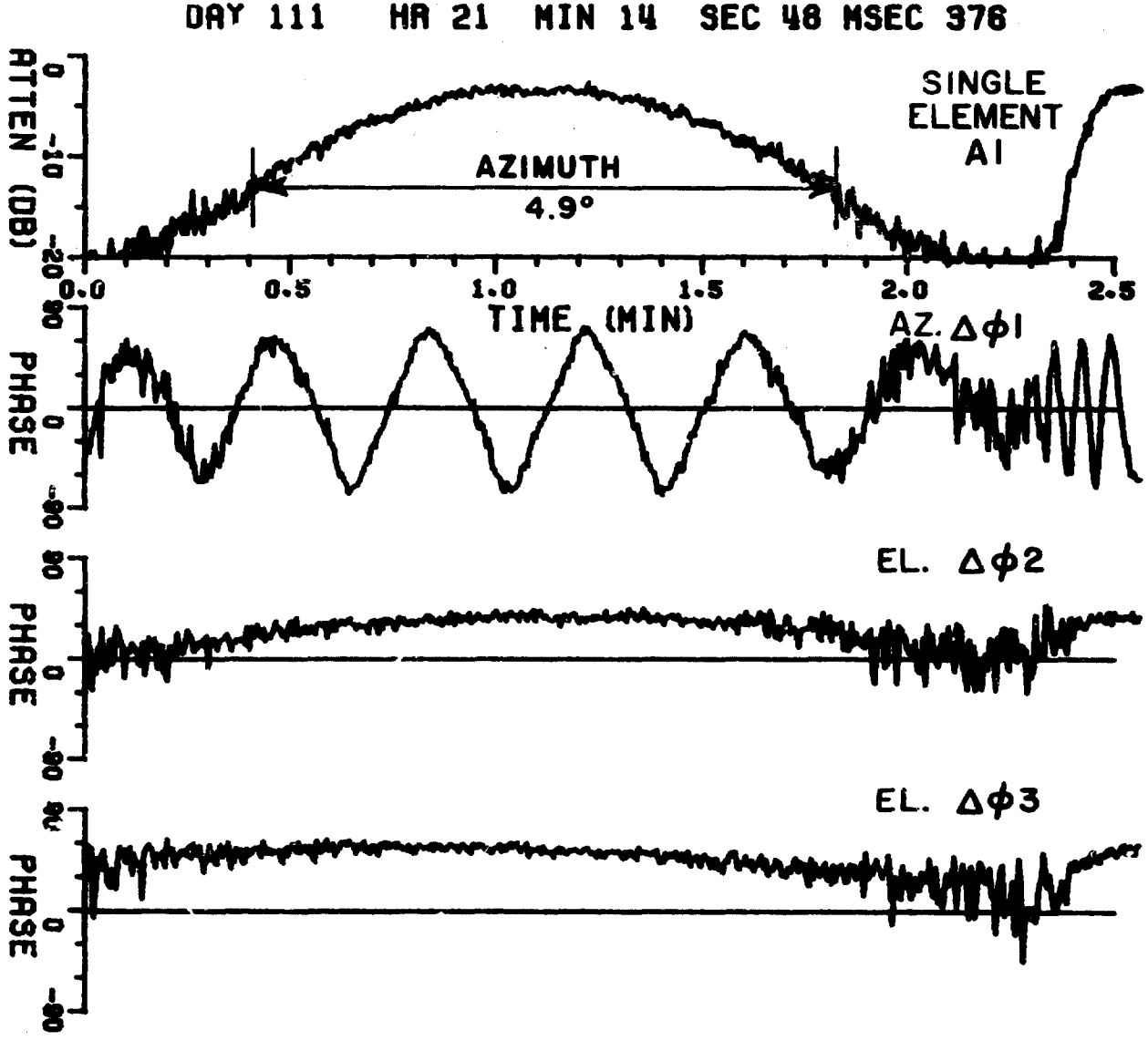

Figure 6. Azimuth amplitude and differential phase pattern.

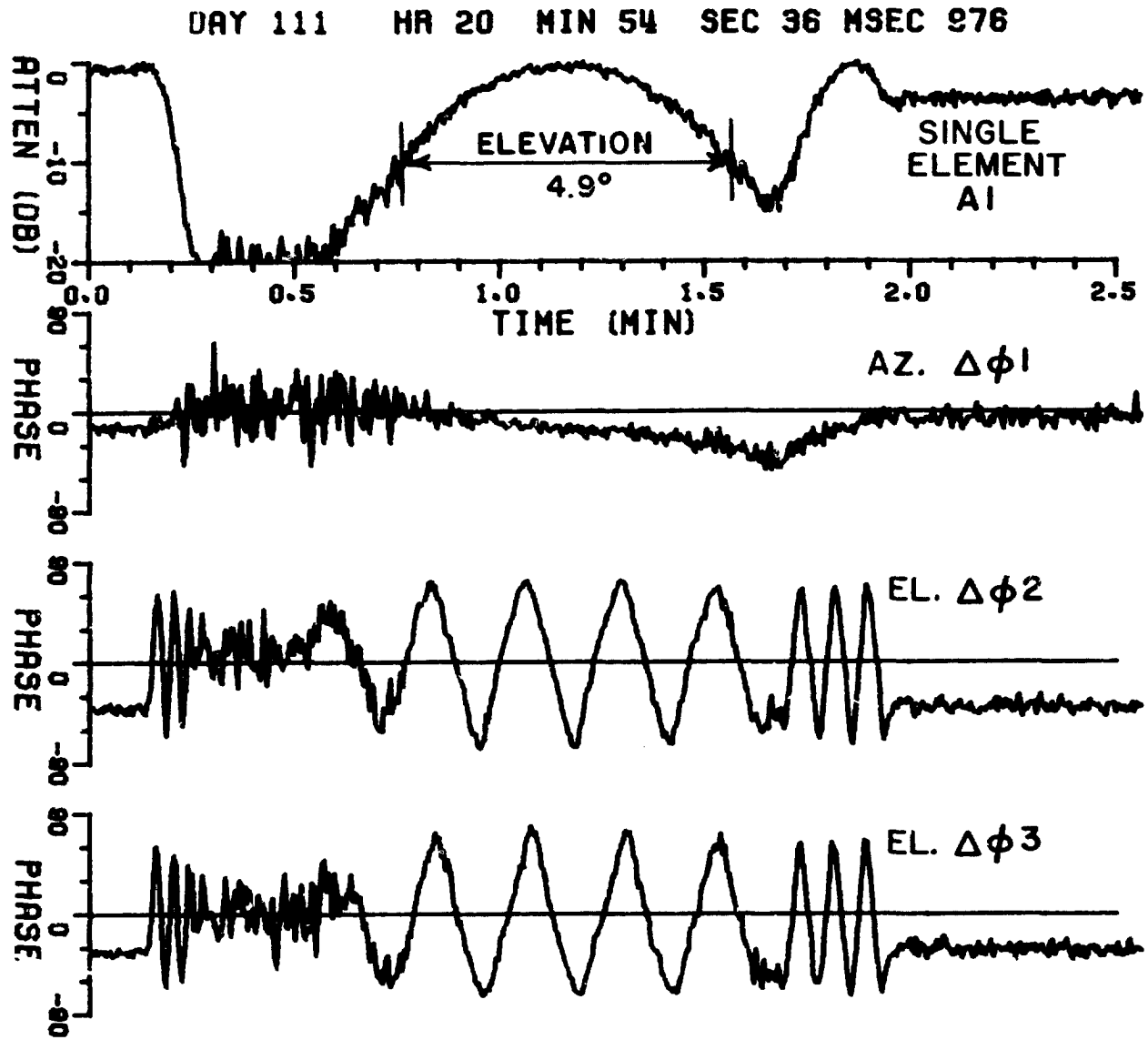

Figure 7. Elevation amplitude and differential phase pattern.

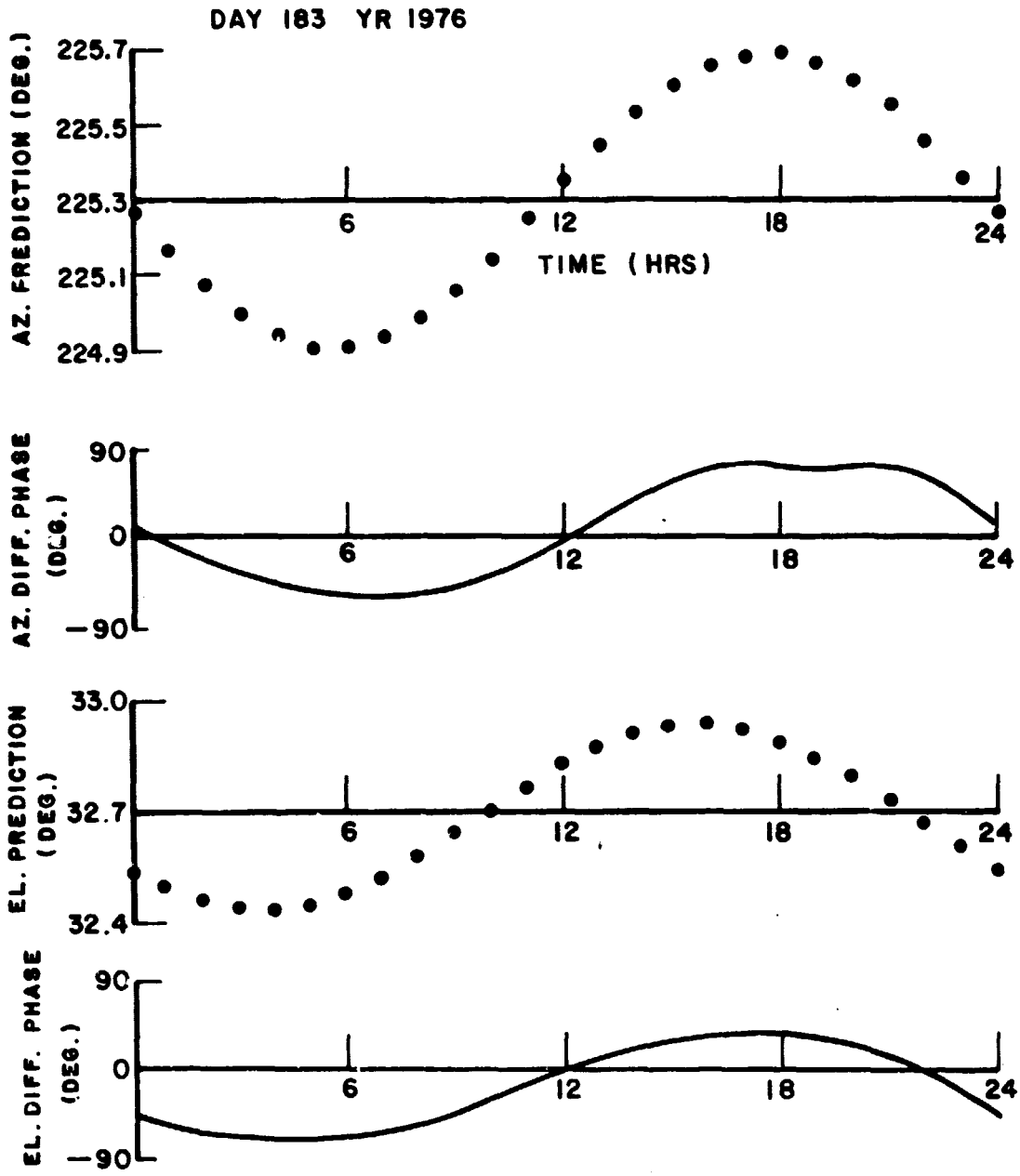

Figure 8. Comparison of predicted azimuth and elevation satellite motion with measured azimuth and elevation differential phase.

satellite (Figure 1). This fact will cause a 1 to 2 dB amplitude variation over a 24 hour period (as an example of this variation note the amplitude channel in Figure 10).

As an additional note on the coherent channel performance of a self-phased array, examine Figure 9. The single element and sum

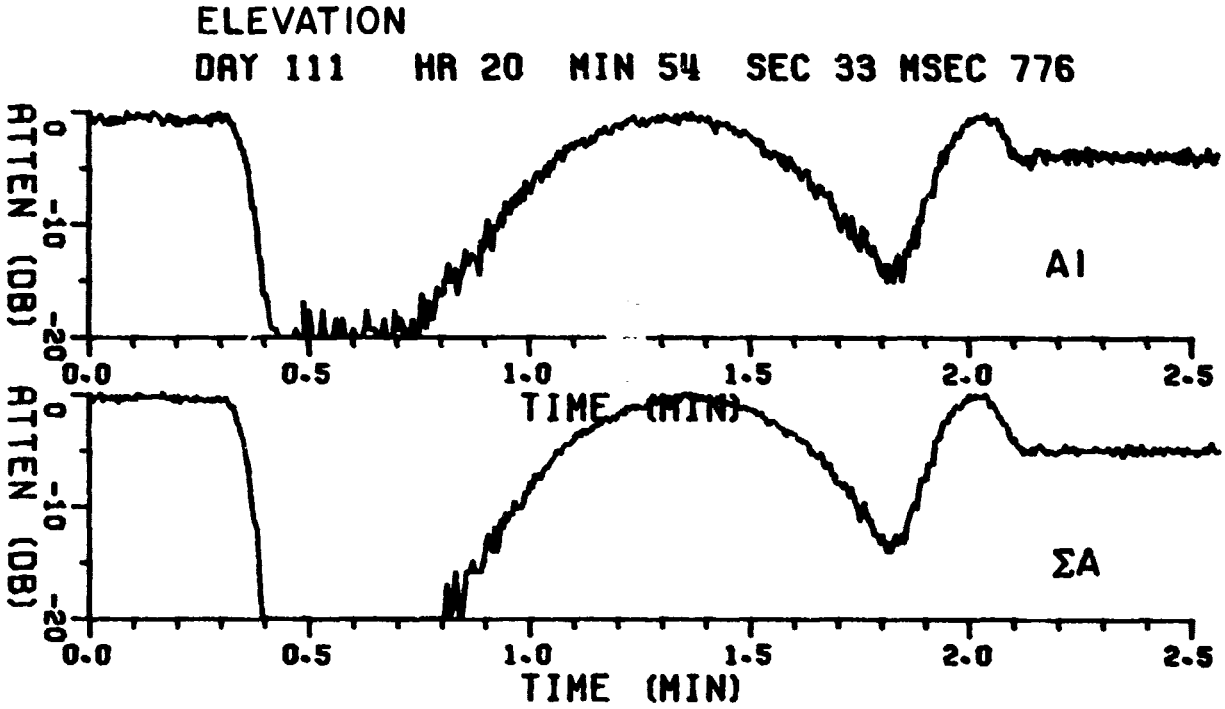

Figure 9. Single element and array sum amplitude comparison.

channel amplitude patterns are plotted for the elevation pattern cut previously described for Figure 7. Because the four elements are self-phased, they maintain coherency as the array is moved off axis in azimuth or elevation. The sum channel thus achieves a 6 dB amplitude improvement compared to a single element over the entire lock range of the array. However, the beamwidth of the sum channel is determined by the individual element patterns and is the same as that of a single element. This behavior is to be expected since the self-phased array pattern varies such that maximum gain occurs in the desired signal direction anywhere within the pattern of a single element; thus, a 6 dB gain improvement is achieved across the entire pattern.

In conclusion, the performance of this self-phased array demonstrates its applicability to angle-of-arrival measurement and to geosynchronous satellite tracking. It eliminates the need for mechanical steering, provides simple unmanned operation, provides gain directly proportional to the number of elements, is insensitive to high wind speeds, and is easily implemented.

V. PROPAGATION DATA

The following examples of propagation data were taken with the array fixed-pointed in the nominal direction of the satellite. The first channel on each plot is a single element amplitude, the second is azimuth differential phase, and the third and fourth are elevation differential phases.

Figure 10 illustrates a day with no significant attenuation events. The diurnal phase variation is comparable to that explained earlier for Figure 8.

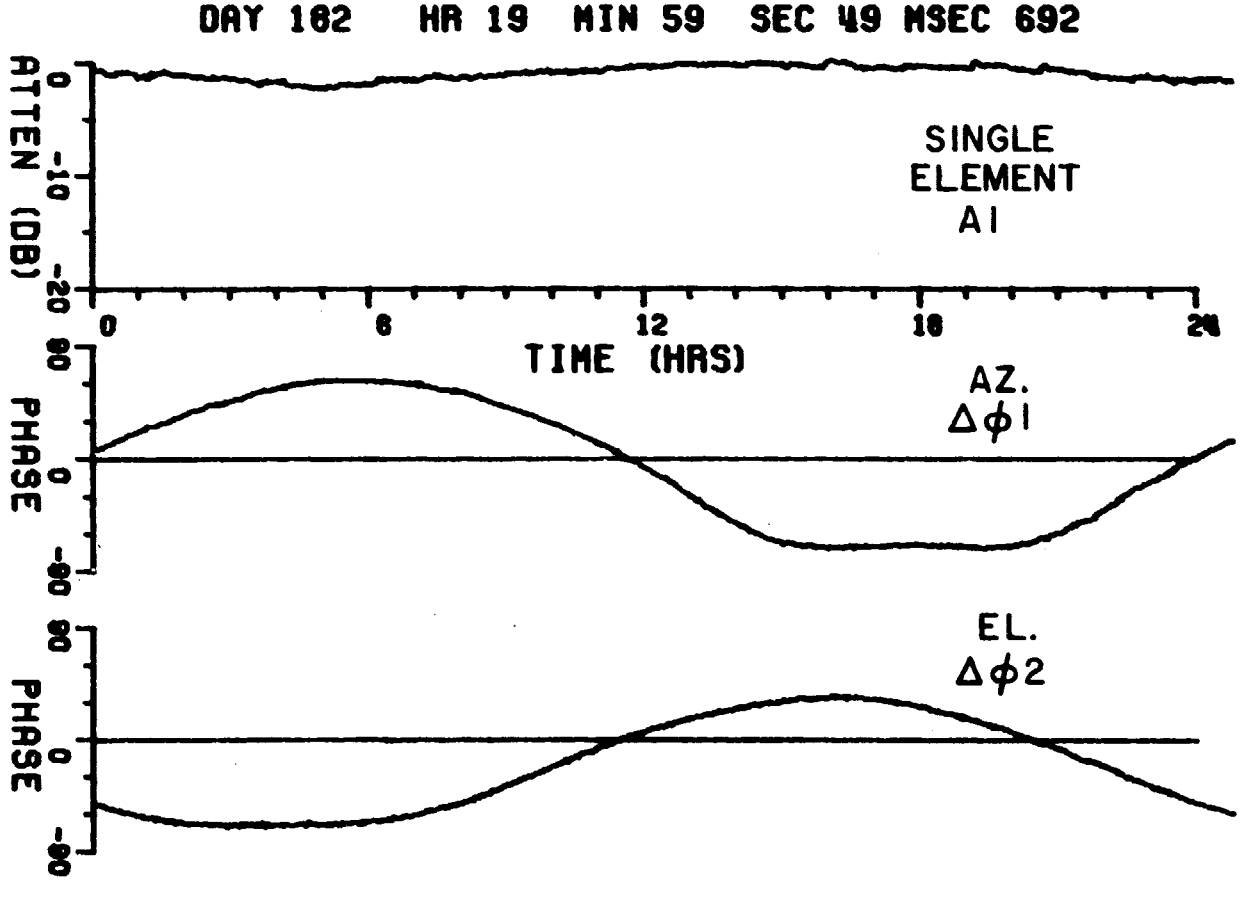

Figure 10. Diurnal amplitude and phase variation.

A precipitation fade event is shown in Figure 11, accompanied by

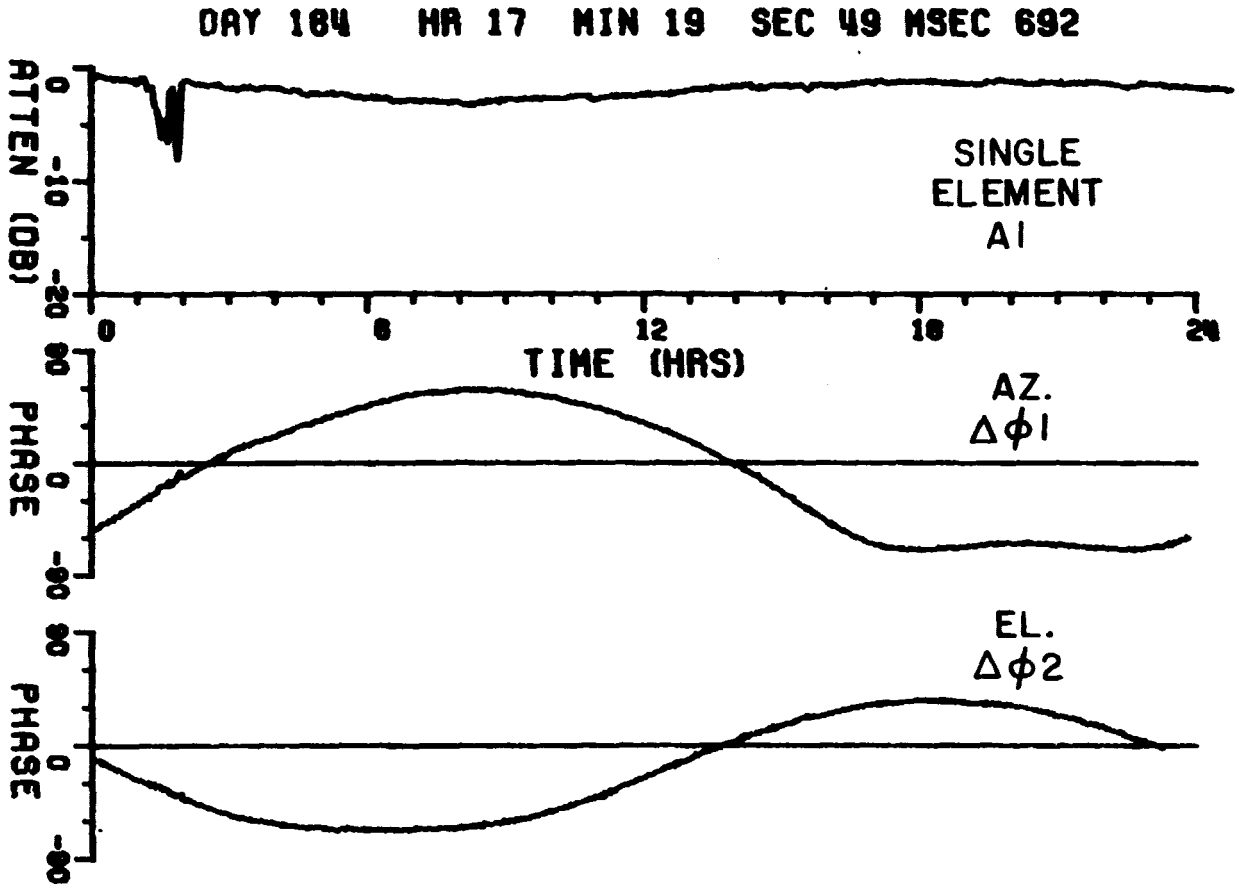

Figure 11. Recorded amplitude and differential phase.

small phase perturbations. The data presented in these 24 hour plots have been averaged over 60 seconds; therefore, even a small departure from the nominal curve represents a significant variation in the parameter being plotted. Figures 12 through 14 are expanded views of a 75 minute period through this event. Preceding and following the event the amplitude variation is on the order of 2 dB peak-to-peak. The azimuth and elevation differential phases for the same time period vary 15° peak-to-peak. During the most intense precipitation periods in Figures 13 and 14 the attenuation reaches about 12 dB and the phase excurisons occasionally exceed 40° peak-to-peak. This phase excursion corresponds to a 0.16° peak-to-peak change in angle-of-arrival. Further statistical analysis is being performed on such data to determine the correlation between azimuth and elevation pair differential phases. In addition, amplitude and phase variance will be examined as a function of time during fade events.

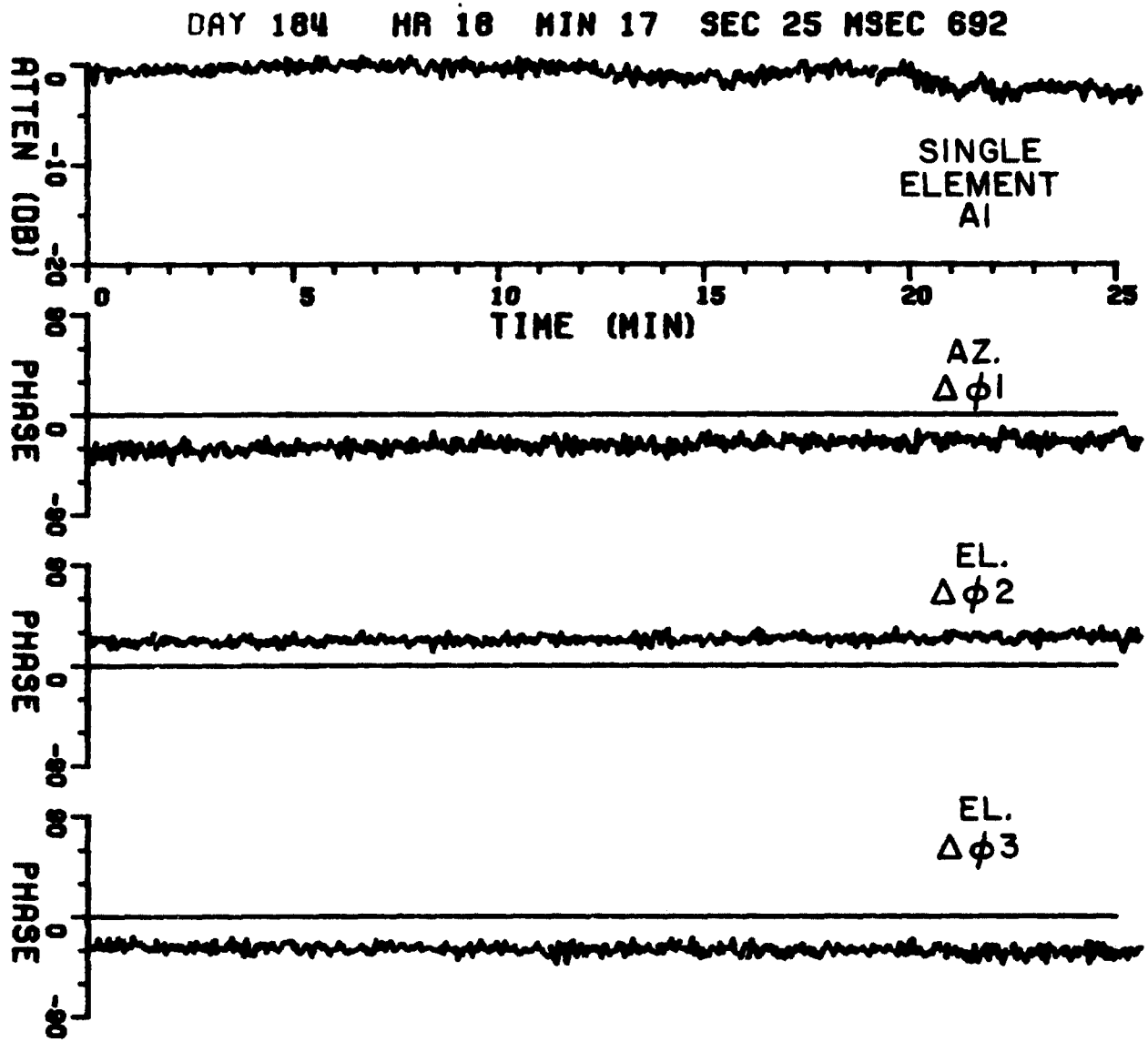

Figure 12. Recorded amplitude and differential phase.

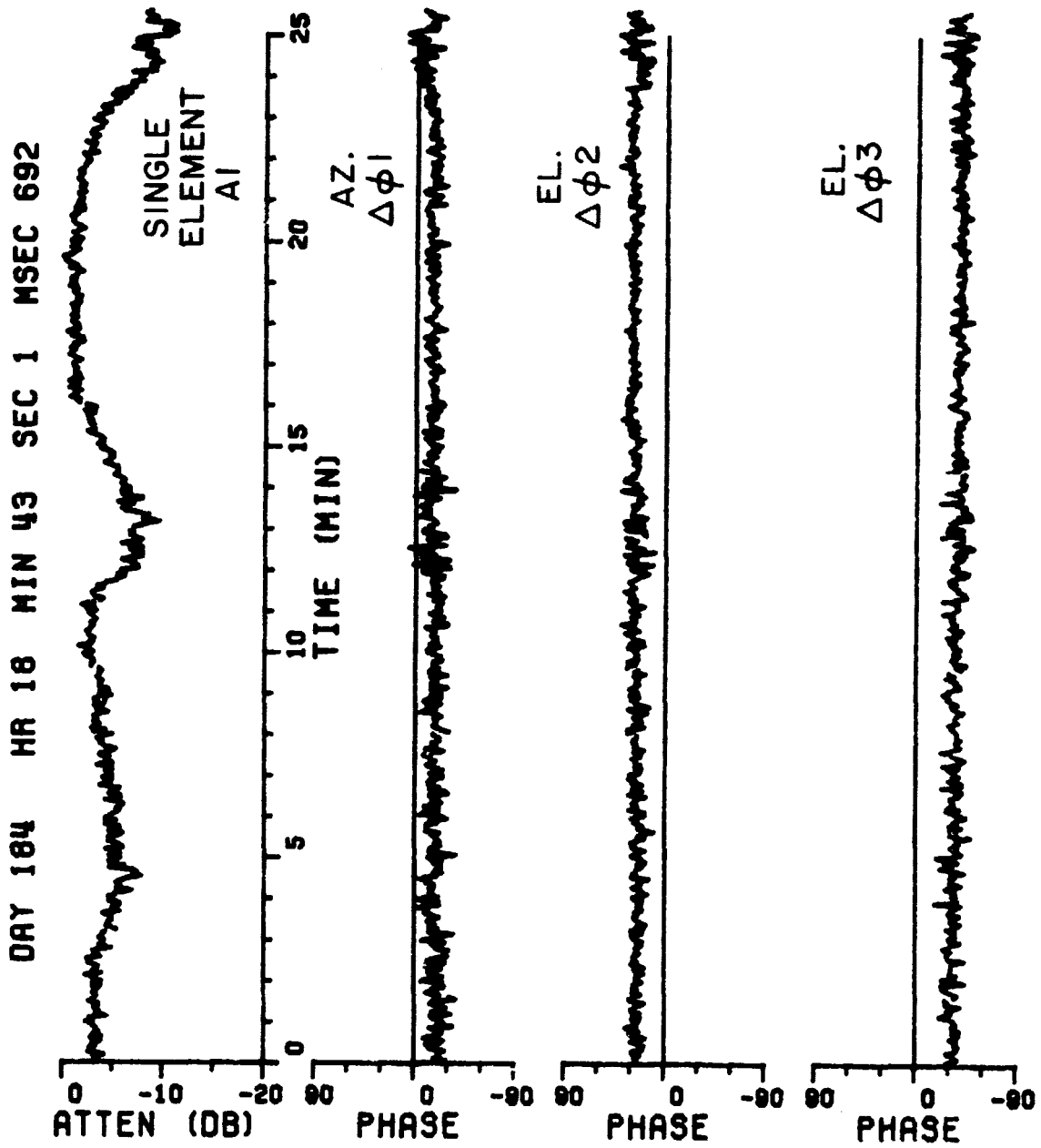

Figure 13. Recorded amplitude and differential phase.

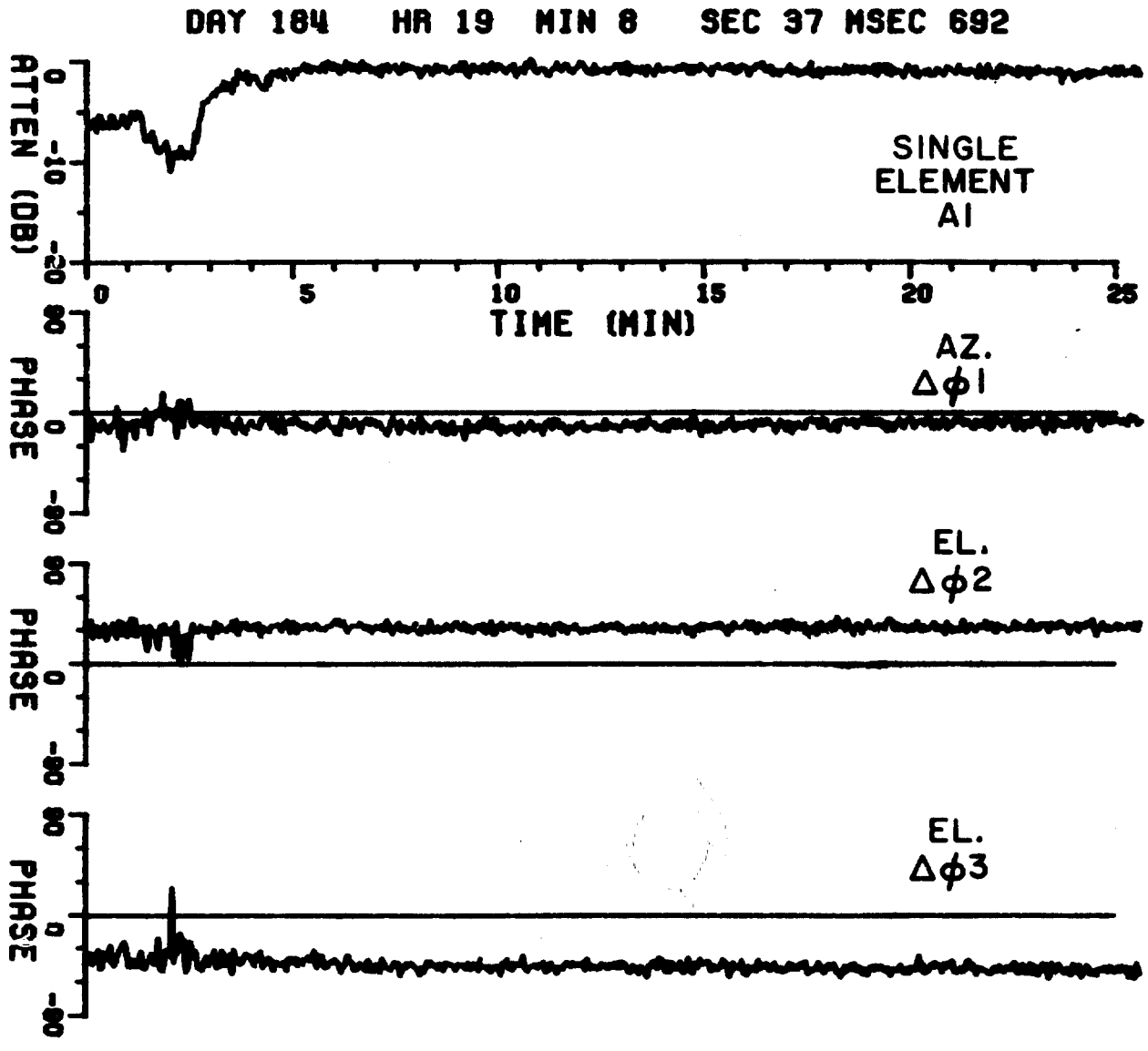

Figure 14. Recorded amplitude and differential phase.

VI. OPERATIONS

The CTS 11.7 GHz beacon signal was first acquired using this system on 20 February 1976. After initial system check-out and debugging the system has been in virtually continuous operation with the exception of brief periods for maintenance, system modifications and improvements, and the CTS eclipse period. A total of 1864 hours of data have been accumulated on digital magnetic tape; these data are currently being processed.

VI. SUMMARY

The performance of the Ohio State University self-phased array has been demonstrated using the 11.7 GHz CTS beacon. This system provides angle-of-arrival as well as amplitude and scintillation statistics. With the present signal to noise ratio, the angle-of-arrival resolution is better than 0.05°.

The technique described here also provides a convenient, non-mechanical method for tracking synchronous satellites with a high gain antenna. The technique has the following characteristics:

- no mechanical steering is required
- readily suited for unmanned operation
- provides gain directly proportional to the number of elements incorporated
- degrades gracefully with front end failure
- insensitive to high wind speeds and buffeting
- can be easily implemented.

REFERENCES

[1] D. B. Hodge, R. C. Taylor and D. M. Theobold, "CTS 11.7 GHz Propagation Experiment-Preliminary Results," presented at the 1976 Annual Meeting USNC/URSI, Amherst, Massachusetts, October 1976.

[2] D. M. Theobold and D. B. Hodge, "ATS-6 Millimeter Wavelength Propagation Experiment," Report 3863-4, April 1975, The Ohio State University ElectroScience Laboratory, Department of Electrical Engineering; prepared under Contract NAS5-21983 for NASA Goddard.

APPENDIX I

DETAILED RECEIVER OPERATION

An expanded block diagram of the CTS self-phased array receiver is shown in Figure A1. The feed package contains the antennas, LHCP feeds, and mixer-amplifiers whose injection is a common 11.67 GHz. The four 30 MHz IF signals enter distribution amplifiers through ±180° phase shifters. These phase shifters are used to compensate for differences in cable lengths so that normal plane wave incidence on the array results in a zero-phase output at all differential phase detectors. The distribution amplifiers are buffers which allow monitoring of the 30 MHz amplitude, frequency, and S/N ratio.

The phase-lock receivers use modified Collins 75S-3 receivers whose 33 MHz and 2.545 MHz injections are provided externally. The 33 MHz is derived from an HP5100A frequency synthesizer, the absolute reference for the entire system, which is accurate to two parts in 10^{11}. The downconverted 3 MHz signals are in turn mixed with a 2.545 MHz VCXO output. This injection point is phase-lock derived and is referred to as the inner-loop reference. The downconverted 455 KHz signals pass through 80 Hz crystal filters which determine the data bandwidth. The filter outputs are buffered by distribution amplifiers and are used in three modules:

1. The inner-loop reference is derived from the 455 KHz receiver output after comparison with a 455 KHz crystal oscillator. This crystal oscillator is common to all elements. A limiter-phase detector and lag filter provides a phase offset control voltage which modulates the 2.545 MHz inner-loop VCXO. The VCXO is controlled such that the signal phase-reference phase difference is minimized. Hence, the four elements phase-lock to a common reference.
2. The four 455 KHz signal outputs, after phase-locking, are coherently summed to provide the array sum output (4).
3. The four 455 KHz signal outputs are amplitude detected as outputs (0-3).

The first mixer injection, 11.67 GHz, is phase-lock derived and is referred to as the outer-loop reference. It is generated by a klystron which is frequency stabilized by a DYMEC synchronizer. One DYMEC reference is the HP5100A and the other is a 10.7 MHz VCXO-output multiplied to 32.1 MHz. The VCXO is controlled in order to track out doppler frequency shift and satellite beacon instability, keeping the signal within the 80 Hz crystal filter bandwidth. The outer-loop control is shown in Figure A2. A window comparator monitors one inner-loop control voltage and steps a voltage control potentiometer. This control voltage provides ultimate klystron frequency control of ±780 Hz in 0.78 Hz increments. The increments are narrow enough so that they do not cause detectable amplitude variations in the data bandwidth.

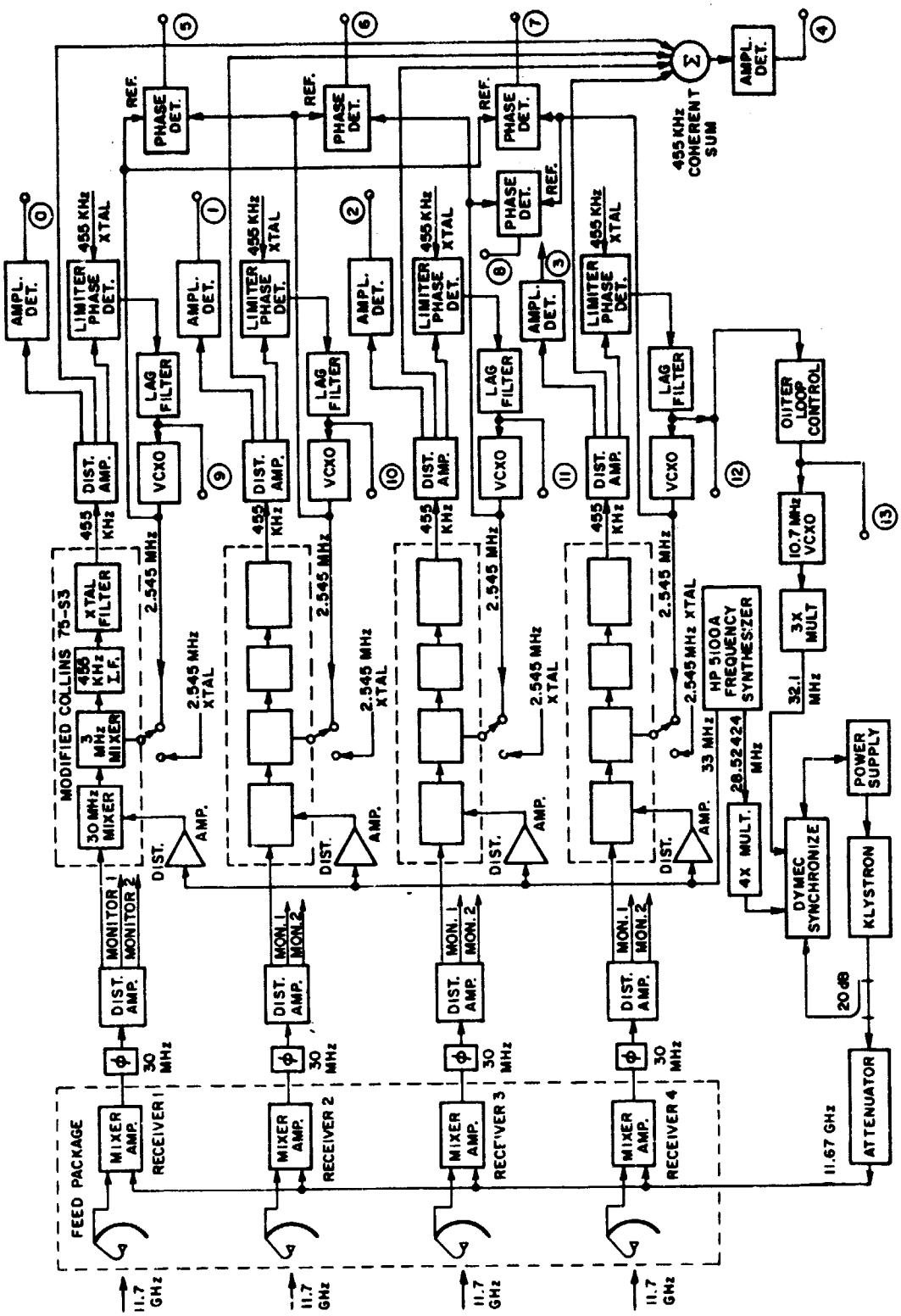

Figure A1. Self-phased array receiver expanded block diagram.

OUTER LOOP CONTROL

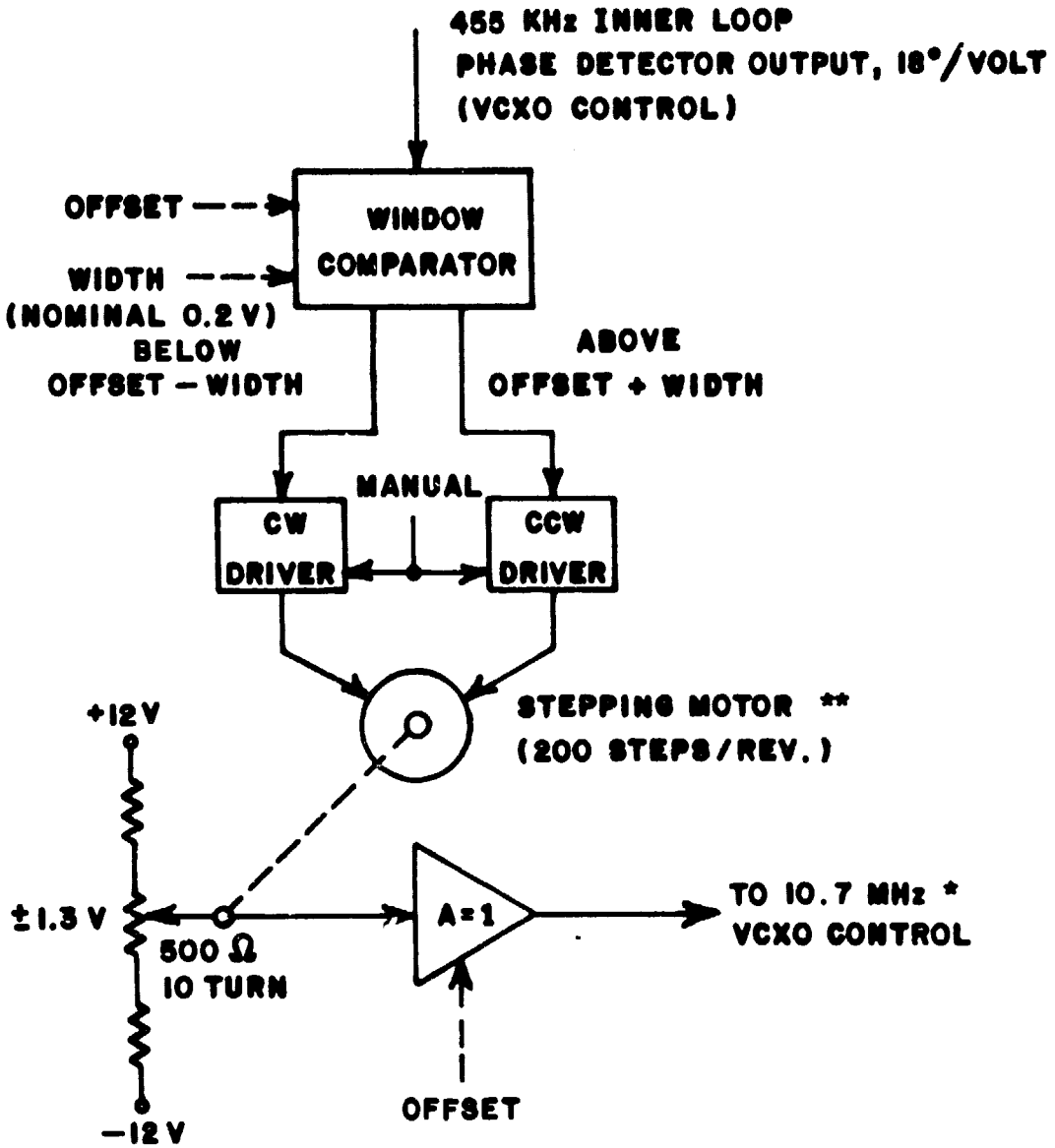

* VCXO sensitivity is 200 Hz/volt or, equivalently 600 Hz/volt at the DYMEC Synchronizer.

** Stepping motor controls the DYMEC over a range of ±780 Hz or, equivalently 0.78 Hz/step.

Figure A2. Outer loop control.

APPENDIX II
DIGITAL DATA FORMAT

Table 1a

Tape Record Format

Header
Sampled Data

Table 1b

Record Type Format

- Type 12 (10 samples/sec) or 13 (1/3 sample/sec)

0	Header from Table 1 Report 3863-4		
15	0	Amplitude 1	1 Amplitude 2
16	2	Amplitude 3	3 Amplitude 4
*	4	Sum Amplitude	5 Diff. Phase 1
	6	Diff. Phase 2	7 Diff. Phase 3
	8	Diff. Phase 4	9 VCXO 1
	10	VCXO 2	11 VCXO 3
	12	VCXO 4	13 Outer Loop Control
	14	Spare	15 Spare
•			
•			

*Repeats a maximum of 32 times in one record; 8 bits bipolar 0-5 volts